Int. J. Mol. Sci. **2005**, *6*, 63-86

International Journal of
Molecular Sciences
ISSN 1422-0067
© 2005 by MDPI
www.mdpi.org/ijms/

Inductive QSAR Descriptors. Distinguishing Compounds with Antibacterial Activity by Artificial Neural Networks

Artem Cherkasov

Division of Infectious Diseases, Faculty of Medicine, University of British Columbia, 2733, Heather street, Vancouver, British Columbia, V5Z 3J5, Canada. Tel. +1-604.875.4588, Fax. +1 604.875.4013; email: artc@interchange.ubc.ca

Received: 20 September 2004; in revised form 14 January 2005 / Accepted: 15 January 2005 / Published: 31 January 2005

Abstract: On the basis of the previous models of inductive and steric effects, 'inductive' electronegativity and molecular capacitance, a range of new 'inductive' QSAR descriptors has been derived. These molecular parameters are easily accessible from electronegativities and covalent radii of the constituent atoms and interatomic distances and can reflect a variety of aspects of intra- and intermolecular interactions. Using 34 'inductive' QSAR descriptors alone we have been able to achieve 93% correct separation of compounds with- and without antibacterial activity (in the set of 657). The elaborated QSAR model based on the Artificial Neural Networks approach has been extensively validated and has confidently assigned antibacterial character to a number of trial antibiotics from the literature.

Keywords: QSAR, antibiotics, descriptors, substituent effect, electronegativity.

Introduction.

Nowadays, rational drug design efforts widely rely on building extensive QSAR models which currently represent a substantial part of modern '*in silico*' research. Due to inability of the fundamental laws of chemistry and physics to directly quantify biological activities of compounds, computational chemists are led to research for simplified but efficient ways of dealing with the phenomenon, such as by the means of molecular descriptors [1]. The QSAR descriptors came to particular demand during last decades when the amounts of chemical information started to grow explosively. Nowadays,

scientists routinely work with collections of hundreds of thousands of molecular structures which cannot be efficiently processed without use of diverse sets of QSAR parameters. Modern QSAR science uses a broad range of atomic and molecular properties varying from merely empirical to quantum-chemical. The most commonly used QSAR arsenals can include up to hundreds and even thousands of descriptors readily computable for extensive molecular datasets. Such varieties of available descriptors in combination with numerous powerful statistical and machine learning techniques allow creating effective and sophisticated structure-bioactivity relationships [1-3]. Nevertheless, although even the most advanced QSAR models can be great predictive instruments, often they remain purely formal and do not allow interpretation of individual factors influencing activity of drugs [3]. Many molecular descriptors (in particular derived from molecular topology alone) lack defined physical justification. The creation of efficient QSAR descriptors also possessing much defined physical meaning still remains one of the most important tasks for the QSAR research.

In a series of previous works we introduced a number of reactivity indices derived from the Linearity of Free Energy Relationships (LFER) principle [4]. All of these atomic and group parameters could be easily calculated from the fundamental properties of bound atoms and possess much defined physical meaning [5-8]. It should be noted that, historically, the entire field of the QSAR has been originated by such LFER descriptors as inductive, resonance and steric substituent constants [4]. As the area progressed further, the substituent parameters remained recognized and popular quantitative descriptors making lots of intuitive chemical sense, but their applicability was limited for actual QSAR studies [9]. To overcome this obstacle, we have utilized the extensive experimental sets of inductive and steric substituent constants to build predictive models for inductive and steric effects [5]. The developed mathematical apparatus not only allowed quantification of inductive and steric interactions between any substituent and reaction centre, but also led to a number of important equations such as those for partial atomic charges [8], analogues of chemical hardness-softness [7] and electronegativity [6].

Notably, all of these parameters (also known as 'inductive' reactivity indices) have been expressed through the very basic and readily accessible parameters of bound atoms: their electronegativities (χ), covalent radii (R) and intramolecular distances (r). Thus, steric Rs and inductive σ^* influence of n -atomic group G on a single atom j can be calculated as:

$$Rs_{G\to j} = \alpha \sum_{i\subset G, i\neq j}^{n} \frac{R_i^2}{r_{i-j}^2} \qquad (1)$$

$$\sigma^*_{G\to j} = \beta \sum_{i\subset G, i\neq j}^{n} \frac{(\chi_i^0 - \chi_j^0)R_i^2}{r_{i-j}^2} \qquad (2)$$

In those cases when the inductive and steric interactions occur between a given atom j and the rest of N-atomic molecule (as sub-substituent) the summation in (1) and (2) should be taken over N-1 terms. Thus, the group electronegativity of *(N-1)*-atomic substituent around atom j has been expressed as the following:

$$\chi^0_{N-1\to j} = \frac{\sum_{i\neq j}^{N-1} \frac{\chi_i^0 (R_i^2 + R_j^2)}{r_{i-j}^2}}{\sum_{i\neq j}^{N-1} \frac{R_i^2 + R_j^2}{r_{i-j}^2}} \quad (3)$$

Similarly we have defined steric and inductive effects of a singe atom onto a group of atoms (the rest of the molecule):

$$Rs_{j\to N-1} = \alpha \sum_{i\neq j}^{N-1} \frac{R_j^2}{r_{j-i}^2} = \alpha R_j^2 \sum_{i\neq j}^{N-1} \frac{1}{r_{j-i}^2} \quad (4)$$

$$\sigma^*_{j\to N-1} = \beta \sum_{i\neq j}^{N-1} \frac{(\chi_j^0 - \chi_i^0) R_j^2}{r_{j-i}^2} = \beta R_j^2 \sum_{i\neq j}^{N-1} \frac{(\chi_j^0 - \chi_i^0)}{r_{j-i}^2} \quad (5)$$

In the works [7, 8] an iterative procedure for calculating a partial charge on *j-th* atom in a molecule has been developed:

$$\Delta N_j = Q_j + \gamma \sum_{i\neq j}^{N-1} \frac{(\chi_j - \chi_i)(R_j^2 + R_i^2)}{r_{j-i}^2} \quad (6)$$

(where Q_j reflects the formal charge of atom *j*).
Initially, the parameter χ in (6) corresponds to χ^0 - an absolute, unchanged electronegativity of an atom; as the iterative calculation progresses the equalized electronegativity χ' gets updated according to (7):

$$\chi' \approx \chi^0 + \eta^0 \Delta N \quad (7)$$

where the local chemical hardness η^0 reflects the "resistance" of electronegativity to a change of the atomic charge. The parameters of 'inductive' hardness η_i and softness s_i of a bound atom *i* have been elaborated as the following:

$$\eta_i = \frac{1}{2\sum_{j\neq i}^{N-1} \frac{R_j^2 + R_i^2}{r_{j-i}^2}} \quad (8)$$

$$s_i = 2\sum_{j\neq i}^{N-1} \frac{R_j^2 + R_i^2}{r_{j-i}^2} \quad (9)$$

The corresponding group parameters have been expressed as

$$\eta_{MOL} = \frac{1}{s_{MOL}} = \frac{1}{2\sum_{j\neq i}^{N-1} \frac{R_j^2 + R_i^2}{r_{j-i}^2}} \quad (10)$$

$$s_{MOL} = \sum_{j\neq i}^{N} \sum_{j\neq i}^{N} \frac{R_j^2 + R_i^2}{r_{j-i}^2} = \sum_{j\neq i}^{N} 2\frac{R_j^2 + R_i^2}{r_{j-i}^2} = \sum_{i}^{N} s_i \quad (11)$$

The interpretation of the physical meaning of 'inductive' indices has been developed by considering a neutral molecule as an electrical capacitor formed by charged atomic spheres [8]. This

approximation related inductive chemical softness and hardness of bound atom(s) with the total area of the facings of electrical capacitor formed by the atom(s) and the rest of the molecule.

We have also conducted very extensive validation of 'inductive' indices on experimental data. Thus, it has been established that R_S steric parameters calculated for common organic substituents form a high quality correlation with Taft's empirical E_S -steric constants ($r^2=0.985$) [10]. The theoretical inductive σ^* constants calculated for *427* substituents correlated with the corresponding experimental numbers with coefficient $r = 0.990$ [5]. The group inductive parameters χ computed by the method (3) have agreed with a number of known electronegativity scales [6]. The inductive charges produced by the iterative procedure (6) have been verified by experimental *C-1s* Electron Core Binding Energies [8] and dipole moments [6]. A variety of other reactivity and physical-chemical properties of organic, organometallic and free radical substances has been quantified within equations (1)-(11) [11-16]. It should be noted, however, that in our previous studies we have always considered different classes of 'inductive' indices (substituent constants, charges or electronegativity) in separate contexts and tended to use the canonical LFER methodology of correlation analysis in dealing with the experimental data. At the same time, a rather broad range of methods of computing 'inductive' indices has already been developed to the date and it is feasible to use these approaches to derive a new class of QSAR descriptors. In the present work we introduce 50 such QSAR descriptors (we called 'inductive') and will test their applicability for building QSAR model of "antibiotic-likeness".

Results

QSAR models for drug-likeness in general and for antibiotic-likeness in particular are the emerging topics of the 'in silico' chemical research. These binary classifiers serve as invaluable tools for automated pre-virtual screening, combinatorial library design and data mining. A variety of QSAR descriptors and techniques has been applied to drug/non-drug classification problem. The latest series of QSAR works report effective separation of bioactive substances from the non-active chemicals by applying the methods of Support Vector Machines (SVM) [17, 18], probability-based classification [19], the Artificial Neural Networks (ANN) [20-22] and the Bayesian Neural Networks (BNN) [23, 24] among others. Several groups used datasets of antibacterial compounds to build the binary classifiers of general antibacterial activity (antibiotic-likeness models) utilizing the ANN algorithm [25-27], linear discriminant analysis (LDA) [28, 29], binary logistic regression [29] or *k*-means cluster method [30]. Thus, in the study [31] the LDA has been used to relate anti-malarial activity of a series of chemical compounds to molecular connectivity QSAR indices. The results clearly demonstrate that creation of QSAR approaches for classification of molecules active against broad range of infective agents represents an important and valuable tack for the modern QSAR research.

Dataset

To investigate the possibility of using the inductive QSAR descriptors for creation an effective model of antibiotic-likeness, we have considered a dataset of Vert and co-authors [27] containing the total of 657 structurally heterogeneous compounds including 249 antibiotics and 408 general drugs.

This dataset has been used in the previous studies [27, 29] and therefore could allow us to comparatively evaluate the performance of QSAR model built upon the inductive descriptors.

Descriptors

50 inductive QSAR descriptors introduced on the basis of formulas (1)-(11) have been described in the greater details in Table 1. Those include various local parameters calculated for certain kinds of bound atoms (for instance for most positively/negatively charges, *etc*), groups of atoms (say, for substituent with the largest/smallest inductive or steric effect within a molecule, *etc*) or computed for the entire molecule. One common feature for all of the introduced inductive descriptors is that they all produce a single value per compound. Another similarity between them is in their relation to atomic electronegativity, covalent radii and interatomic distances. It should also be noted, that all descriptors (except the total formal charge) depend on the actual spatial structure of molecules. The choice of particular inductive descriptors in Table 1 was driven by our expectation to have a limited set of QSAR parameters reflecting the greatest variety of different aspects of intra- and intermolecular interactions a molecule can be engaged into. It should be mentioned, however, that some inductive descriptors may reflect related or similar molecular/atomic properties and therefore can be correlated in certain cases (even though the analytical representation of those descriptors does not directly imply their co-linearity). Thus, a special precaution should be taken when using such parameters for QSAR modeling. The procedure of selection of appropriate inductive descriptors has been outlined in the following section.

Table 1. Inductive QSAR descriptors introduced on the basis of equations (1)-(11).

Descriptor	**Characterization**	**Parental formula(s)**
χ (electronegativity) – based		
EO_Equalized[a]	Iteratively equalized electronegativity of a molecule	Calculated iteratively by (7) where charges get updated according to (6); an atomic hardness in (7) is expressed through (8)
Average_EO_Pos[a]	Arithmetic mean of electronegativities of atoms with positive partial charge	$\frac{\sum_{i}^{n^+}\chi_i^0}{n^+}$ where n^+ is the number of atoms $\underline{i}$ in a molecule with positive partial charge
Average_EO_Neg[a]	Arithmetic mean of electronegativities of atoms with negative partial charge	$\frac{\sum_{i}^{n^-}\chi_i^0}{n^-}$ where n^- is the number of atoms $\underline{i}$ in a molecule with negative partial charge
η (hardness) – based		
Global_Hardness[a]	Molecular hardness - reversed softness of a molecule	(10)
Sum_Hardness[a]	Sum of hardnesses of atoms of a molecule	Calculated as a sum of inversed atomic softnesses in turn computed within (9)
Sum_Pos_Hardness[a]	Sum of hardnesses of atoms with positive partial charge	Obtained by summing up the contributions from atoms with positive charge computed by (8)

Table 1. Cont.

Sum_Neg_Hardness[a]	Sum of hardnesses of atoms with negative partial charge	Obtained by summing up the contributions from atoms with negative charge computed by (8)
Average_Hardness[a]	Arithmetic mean of hardnesses of all atoms of a molecule	Estimated by dividing quantity (10) by the number of atoms in a molecule
Average_Pos_Hardness	Arithmetic mean of hardnesses of atoms with positive partial charge	$\frac{\sum_i^{n^+} \eta_i}{n^+}$ where n^+ is the number of atoms i with positive partial charge.
Average_Neg_Hardness[a]	Arithmetic mean of hardnesses of atoms with negative partial charge	$\frac{\sum_i^{n^-} \eta_i}{n^-}$ where n^- is the number of atoms i with negative partial charge.
Smallest_Pos_Hardness[a]	Smallest atomic hardness among values for positively charged atoms	(8)
Smallest_Neg_Hardness[a]	Smallest atomic hardness among values for negatively charged atoms.	(8)
Largest_Pos_Hardness	Largest atomic hardness among values for positively charged atoms	(8)
Largest_Neg_Hardness	Largest atomic hardness among values for negatively charged atoms	(8)
Hardness_of_Most_Pos	Atomic hardness of an atom with the most positive charge	(8)
Hardness_of_Most_Neg[a]	Atomic hardness of an atom with the most negative charge	(8)
s (softness) - based		
Global_Softness	Molecular softness – sum of constituent atomic softnesses	(11)
Total_Pos_Softness[a]	Sum of softnesses of atoms with positive partial charge	Obtained by summing up the contributions from atoms with positive charge computed by (9)
Total_Neg_Softness[a]	Sum of softnesses of atoms with negative partial charge	Obtained by summing up the contributions from atoms with negative charge computed by (9)
Average_Softness	Arithmetic mean of softnesses of all atoms of a molecule	(11) divided by the number of atoms in molecule
Average_Pos_Softness	Arithmetic mean of softnesses of atoms with positive partial charge	$\frac{\sum_i^{n^+} s_i}{n^+}$ where n^+ is the number of atoms i with positive partial charge.
Average_Neg_Softness	Arithmetic mean of softnesses of atoms with negative partial charge	$\frac{\sum_i^{n^-} s_i}{n^-}$ where n^- is the number of atoms i with negative partial charge.

Table 1. Cont.

Smallest_Pos_Softness[a]	Smallest atomic softness among values for positively charged atoms	(9)
Smallest_Neg_Softness[a]	Smallest atomic softness among values for negatively charged atoms	(9)
Largest_Pos_Softness	Largest atomic softness among values for positively charged atoms	(9)
Largest_Neg_Softness	Largest atomic softness among values for positively charged atoms	(9)
Softness_of_Most_Pos[a]	Atomic softness of an atom with the most positive charge	(9)
Softness_of_Most_Neg[a]	Atomic softness of an atom with the most negative charge	(9)
q (charge)- based		
Total_Charge	Sum of absolute values of partial charges on all atoms of a molecule	$\sum_i^N \lvert\Delta N_i\rvert$ where all the contributions ΔN_i derived within (6)
Total_Charge_Formal[a]	Sum of charges on all atoms of a molecule (formal charge of a molecule)	Sum of all contributions (6)
Average_Pos_Charge[a]	Arithmetic mean of positive partial charges on atoms of a molecule	$\frac{\sum_i^{n^+} \Delta N_i}{n^+}$ where n^+ is the number of atoms $\underline{i}$ with positive partial charge
Average_Neg_Charge[a]	Arithmetic mean of negative partial charges on atoms of a molecule	$\frac{\sum_i^{n^-} \Delta N_i}{n^-}$ where n^- is the number of atoms $\underline{i}$ with negative partial charge
Most_Pos_Charge[a]	Largest partial charge among values for positively charged atoms	(6)
Most_Neg_Charge	Largest partial charge among values for negatively charged atoms	(6)
σ (inductive parameter) – based*		
Total_Sigma_mol_i[a]	Sum of inductive parameters *σ*(molecule→atom)* for all atoms within a molecule	$\sum_i^N \sigma^*_{G\to i}$ where contributions $\sigma^*_{G\to i}$ are computed by equation (2) with *n=N-1* – i.e. each atom *j* is considered against the rest of the molecule *G*
Total_Abs_Sigma_mol_i	Sum of absolute values of group inductive parameters *σ*(molecule→atom)* for all atoms within a molecule	$\sum_i^N \lvert\sigma^*_{G\to i}\rvert$

Table 1. Cont.

Most_Pos_Sigma_mol_i[a]	Largest positive group inductive parameter *σ*(molecule→atom)* for atoms in a molecule	(2)
Most_Neg_Sigma_mol_i[a]	Largest (by absolute value) negative group inductive parameter *σ*(molecule→atom)* for atoms in a molecule	(2)
Most_Pos_Sigma_i_mol[a]	Largest positive atomic inductive parameter *σ*(atom→molecule)* for atoms in a molecule	(5)
Most_Neg_Sigma_i_mol[a]	Largest negative atomic inductive parameter *σ*(atom→molecule)* for atoms in a molecule	(5)
Sum_Pos_Sigma_mol_i	Sum of all positive group inductive parameters *σ*(molecule →atom)* within a molecule	$\sum_{i}^{n^+}\lvert\sigma^*_{G\to i}\rvert$ where $\sigma^*_{G\to i}>0$ and n^+ is the number of *N-1* atomic substituents in a molecule with positive inductive effect (electron acceptors)
Sum_Neg_Sigma_mol_i[a]	Sum of all negative group inductive parameters *σ*(molecule →atom)* within a molecule	$\sum_{i}^{n^-}\lvert\sigma^*_{G\to i}\rvert$ where $\sigma^*_{G\to i}<0$ and n^- is the number of *N-1* atomic substituents in a molecule with negative inductive effect (electron donors)
Rs (steric parameter) – based		
Largest_Rs_mol_i[a]	Largest value of steric influence *Rs(molecule→atom)* in a molecule	(1) where *n=N-1* - each atom *j* is considered against the rest of the molecule *G*
Smallest_Rs_mol_i[a]	Smallest value of group steric influence *Rs(molecule→atom)* in a molecule	(1) where *n=N-1* - each atom *j* is considered against the rest of the molecule *G*
Largest_Rs_i_mol	Largest value of atomic steric influence *Rs(atom→molecule)* in a molecule	(4)
Smallest_Rs_i_mol[a]	Smallest value of atomic steric influence *Rs(atom→molecule)* in a molecule	(4)
Most_Pos_Rs_mol_i[a]	Steric influence *Rs(molecule→atom)* ON the most positively charged atom in a molecule	(1)
Most_Neg_Rs_mol_i[a]	Steric influence *Rs(molecule→atom)* ON the most negatively charged atom in a molecule	(1)

Table 1. Cont.

Most_Pos_Rs_i_mol	Steric influence *Rs(atom→molecule)* OF the most positively charged atom to the rest of a molecule	(4)
Most_Neg_Rs_i_mol[a]	Steric influence *Rs(atom→molecule)* OF the most negatively charged atom to the rest of a molecule	(4)

[a] – descriptors selected for building the antibiotic-likeness QSAR model.

Selection of variables

To build a binary QSAR model enabling effective separation of antibacterials we have initially calculated all 50 individual inductive descriptors for each molecule from the Vert's dataset. We have used the hydrogen suppressed representation of the molecular structures – *i.e.* only the heavy atoms have been taken into account. The inductive QSAR descriptors have been calculated within the MOE package [32] from values of atomic electronegativities and radii taken from our previous publications [5]. To avoid the mentioned cross-correlation among the independent variables we have computed pair wise regressions between all 50 sets of the QSAR parameters and removed those inductive descriptors which formed any linear dependence with $R \geq 0.9$. As the result of this procedure, only 34 inductive QSAR descriptors have been selected for the further processing (see the legend to Table 1). The average values of these 34 parameters independently calculated for antibacterial and non- antibacterial compounds have been plotted onto Figure 1. As it can be seen, the corresponding curves for two classes of compounds are clearly separated on the graph and, hence, the selected 34 inductive descriptors should allow building an effective QSAR model of "antibiotic likeness".

Figure 1. Averaged values of 34 selected inductive QSAR descriptors calculated independently within studied sets of antibiotics (dashed line) and non-antibiotics (solid line).

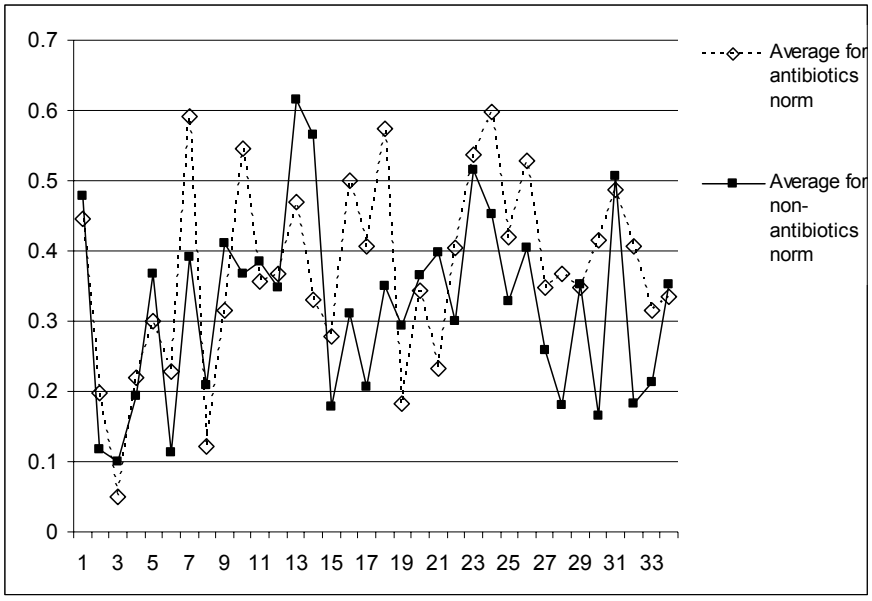

QSAR model

In order to relate the inductive descriptors to antibiotic activity of the studied molecules we have employed the Artificial Neural Networks (ANN) method – one of the most effective pattern recognition techniques. During the last decades the machine-learning approaches have became an essential part of the QSAR research; the detailed description of the ANN's fundamentals can be found in numerous sources [33 for example].

In our study we have used the standard back-propagation ANN configuration consisting of 34 input and 1 output nodes. The number of nodes in the hidden layer was varied from 2 to 14 in order to find the optimal network that allows most accurate separation of antibacterials from other compounds in the training sets. For effective training of the ANN (to avoid its over fitting) we have used the training sets of 592 compounds (including 197 antibiotics) randomly derived as 90 percent of the total of 657 molecules. In each training run the remaining 10 percents of the compounds were used as the testing set to assess the predictive ability of the model. It should be noted, that we the condition of non-correlation amongst the descriptors has been monitored within the training and the testing sets of compounds as well.

During the learning phase, a value of 1 has been assigned to the training set's molecules possessing antibacterial activity and value 0 to the others. For each configuration of the ANN (with 2, 3, 4, 6, 8, 10, 12, and 14 hidden nodes respectively) we have conducted 20 independent training runs to evaluate the average predictive power of the network. Table 2 contains the resulting values of specificity, sensitivity and accuracy of separation of antibacterial and non-antibacterial compounds in the testing sets. The corresponding counts of the false/true positive- and negative predictions have been estimated using 0.4 and 0.6 cut-off values for non-antibacterials and antibacterials respectively. Thus, an antibiotic compound from the testing set, has been considered correctly classified by the ANN only when its output value ranged from 0.6 to 1.0. For each non-antibiotic entry of the testing set the correct classification has been assumed if the corresponding ANN output lay between 0 and 0.4. Thus, all network output values ranging from 0.4 to 0.6 have been ultimately considered as incorrect predictions (rather than undetermined or non-defined).

Table 2. Parameters of specificity, sensitivity, accuracy and positive predictive values for prediction of antibiotic and non-antibiotic compounds by the artificial neural networks with the varying number of hidden nodes. The cut-off values 0.4 and 0.6 have been used for negative and positive predictions respectively.

Hidden nodes	Specificity	Sensitivity	Accuracy	PPV
2	0.8	0.92	0.846	0.751
3	0.926	0.928	0.923	0.884
4	0.925	0.92	0.923	0.884
6	0.9	1	0.938	0.862
8	0.9	0.92	0.907	0.851
10	0.9	0.92	0.907	0.851
12	0.9	0.92	0.907	0.851
14	0.815	1	0.923	0.833

Considering that one of the most important implications for the "antibiotic-likeness" model is its potential use for identification of novel antibiotic candidates from electronic databases, we have calculated the parameters of the Positive Predictive Values (PPV) for the networks while varying the number of hidden nodes. Taking into account the PPV values for the networks with the varying number of the hidden nodes along with the corresponding values of sensitivity, specificity and general accuracy we have selected neural network with three hidden nodes as the most efficient among the studied. The ANN with 34 input-, 3 hidden- and 1 output nodes has allowed the recognition of 93% of antibiotic and 93% of non-antibiotic compounds, on average. The output from this 34-3-1 network has also demonstrated very good separation on positive (antibiotics) and negative (non-antibiotics) predictions. Figure 2 features frequencies of the output values for the training and testing sets consisting of ⅓ of antibiotic and ⅔ of non-antibiotics compounds. As it can readily be seen from the graph, the vast majority of the predictions has been contained within [0.0÷0.4] and [0.6÷1.0] ranges what also illustrates that 0.4 and 0.6 cut-offs values provide very adequate separation of two bioactivity classes (Tables 3 and 4 feature the outputs values from the 34-3-1 ANN for the training and testing sets respectively).

Figure 2. Distribution of the output values from the ANN with three nodes in the hidden layer and trained on the set containing 90% of the studied compounds

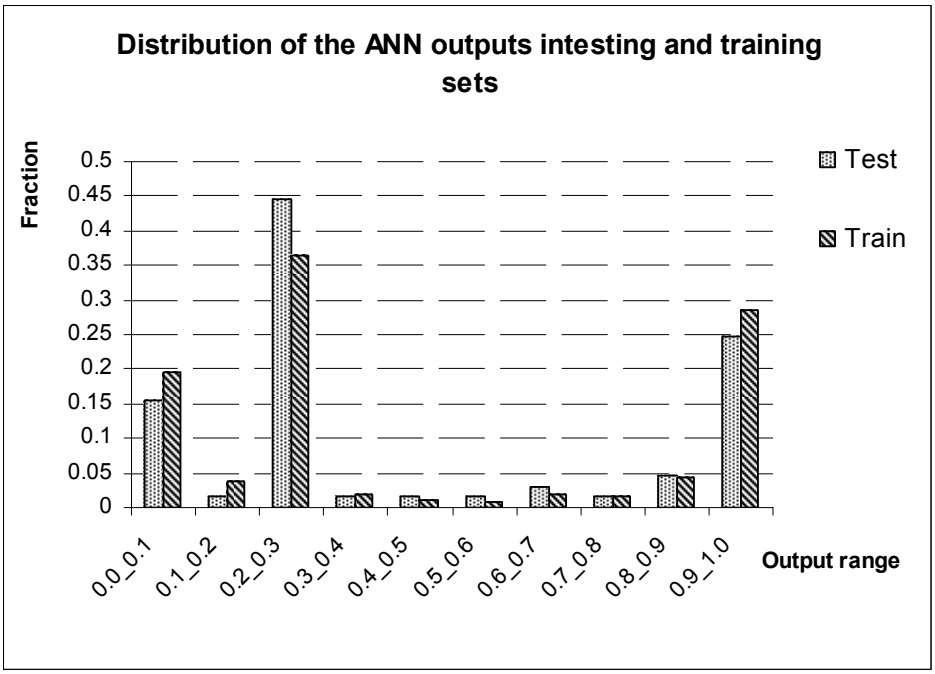

It should be mentioned, that the estimated 93% accuracy of the prediction by the 34-3-1 ANN is similar or superior to the results by several similar 'antibiotic-likeness' studies where the overall cross—validated accuracy can range from 78 [20] to 98% [26] depending of the QSAR methodology, size of antibiotics/non-antibiotics dataset, cross-correlation technique and statistics utilized.

We have also applied the developed techniques on the non-hydrogen suppressed molecular structures. The estimated accuracy of antibiotic/non-antibiotic classification was very close to the

results for the hydrogen suppressed molecules. In contrast, the time for the calculation of the inductive QSAR descriptors in the former case is much shorter as the total number of all atoms nearly doubles.

Discussion

The accuracy of discrimination of antibiotic compounds by the artificial neural networks built upon the 'inductive' descriptors clearly demonstrates an adequacy and good predictive power of the developed QSAR model. There is strong evidence, that the introduced inductive descriptors do adequately reflect the structural properties of chemicals, which are relevant for their antibacterial activity. This observation is not surprising considering that the inductive QSAR descriptors calculated within (1)–(11) should cover a very broad range of proprieties of bound atoms and molecules related to their size, polarizability, electronegativity, compactness, mutual inductive and steric influence and distribution of electronic density, *etc*. The results of the study demonstrate that not extensive sets of inductive QSAR descriptors having much defined physical meaning can be sufficient for creating useful models of "antibiotic-likeness". The accuracy of the developed QSAR model is superior or similar compared to other binary classifiers on the same set of molecules but using much more extensive collections of QSAR descriptors [27, 29].

Presumably, accuracy of the approach operating by the inductive descriptors can be improved even further by expanding the QSAR descriptors or by applying more powerful classification techniques such as Support Vector Machines or Bayesian Neural Networks. Use of merely statistical techniques in conjunction with the inductive QSAR descriptors would also be beneficial, as they will allow interpreting individual descriptor contributions into molecular "antibiotic-likeness". The selection of drugs used for the simulation can also be extended and/or refined. For instance, it has been experimentally confirmed that several non-antibacterial compounds from Vert's dataset can, in fact, possess definite antibacterial activity. Thus, anti-inflammatory drugs diclofenac [34, 35], piroxicam, mefenamic acid and naproxen [35], antihistamines – bromodiphenhydramine [36] diphenhydramine [36] and triprolidine [37], anti-psychotics – chlorpromazine [38, 39] and fluphenazine [40, 41], the tranquilizer promazine [42] and anti-hypertensive methyldopa [43] all exhibit moderate to powerful potential against microbes. It is obvious, that having all these compounds as the negative control can interfere with the training of efficient antibiotic-likeness model. We, however, did not remove these substances from the e training and testing sets for the sake of comparison of our results with the previous data. Nonetheless, despite the certain drawbacks, it is obvious that the developed ANN-based QSAR model operating by the inductive descriptors has demonstrated very high accuracy and can be used for mining electronic collections of chemical structures for novel antibiotic candidates.

An application of the model

We have decided to test the developed model of "antibiotic-likeness" on the series of early-stage antibiotic compounds featured in the free issue of the Drug Data Report – a journal presenting preliminary drug research results appearing for the first time in patent literature [44]. The "experimental" antibiotic compounds cited by the issue included one penicillin- and two cephalosporin- derivatives as well as a number of high molecular weight chemicals with complex

spatial structures such as five C11-carbamate azalides and four eremomycin carboxamides (the corresponding structural formulas are presented on Figure 3).

Figure 3. Chemical structures of twelve early stage antibiotics from the Drug Data Report used for validation for the developed ANN – based QSAR model.

3a)

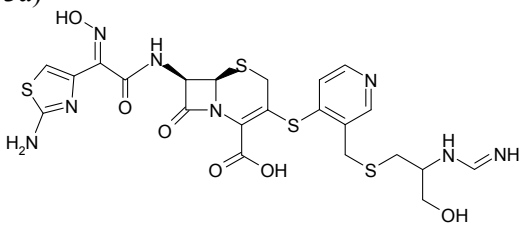

286547

3b)

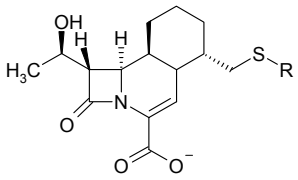

286848: R = C(S)N(C_2H_5)C_6H_5

286847: R = 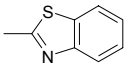

3c)

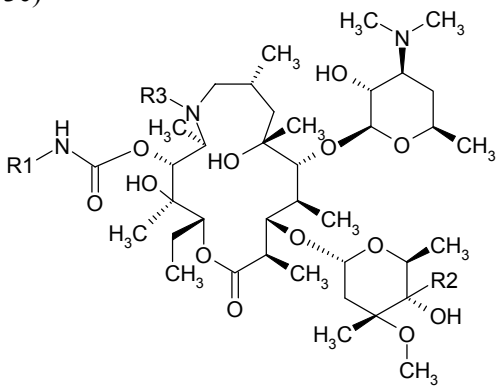

286724: **R1** = 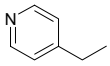 **R2** = H **R3** = CH_3

286724: **R1** = 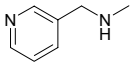 **R2** = H **R3** = CH_3

286726: **R1** = 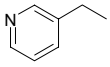 **R2** = 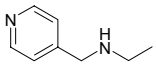 **R3** = CH_3

286727: **R1** = 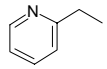 **R2** = H **R3** = CH_2CH_3

286728: **R1** = 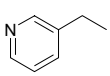 **R2** = H **R3** = $CH_2CH{=}CH_2$

3d)

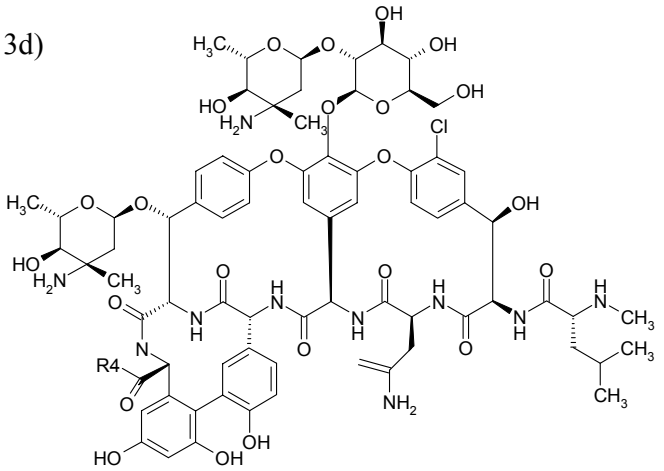

287132: **R4** = NH-$(CH_2)_9CH_3$

287133: **R4** = (S)-$N(CH_2)_4$-$CH(NH_2)CONHC_{10}H_{21}$

287135: **R4** = 4-$(C_{10}H_{21})$-1-Piz

287136: **R4** = 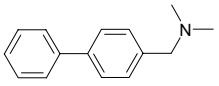

For each of 12 compounds from the validation set we have calculated 34 inductive descriptors used earlier. The normalized patterns of the independent variables have then been passed through 34-3-1 network with its node–associated weights pre-assigned during the training. The ANN has produced the output parameters presented in Table 5. As it can be seen from the data, all of the estimated output values score well above 0.60 threshold what confidently assigns all of the trial molecules to the class of antibiotics.

Table 3. Compounds of the training set and output values from the trained neural network with three hidden nodes.

Name	Output		Name	Output
antibiotics			apicycline	0.975
4'-(methylsulfamoyl)sulfanilanilide	0.973		apramycin	0.980
4'-formylsuccinanilic acid			azidocillin	0.979
thiosemicarbazone	0.259		arbekacin	0.980
4-sulfanilamidosalicylic acid	0.938		aspoxicillin	0.975
acediasulfone	0.828		azidamfenicol	0.966
acetyl sulfamethoxypyrazine	0.855		azlocillin	0.850
acetyl sulfisoxazole	0.964		aztreonam	0.981
amidinocillin	0.702		bacampicillin	0.982
amidinocillin pivoxil	0.938		benzylpenicillinic acid	0.924
amifloxacin	0.881		benzylsulfamide	0.733
amikacin	0.984		biapenem	0.830
apalcillin	0.981		brodimoprim	0.585

Table 3. Cont.

Name	Output		Name	Output
butirosin	0.984		cephalothin	0.977
carbenicillin	0.974		cephapirin sodium	0.984
carfecillin sodium	0.970		cephradine	0.897
carindacillin(a,e,f,i)	0.938		chloramphenicol	0.606
carumonam	0.985		chloramphenicol palmitate	0.604
cefaclor	0.860		chloramphenicol pantothenate	0.983
cefadroxil	0.915		chlortetracycline	0.984
cefamandole	0.964		cinoxacin	0.770
cefatrizine	0.973		clinafloxacin	0.920
cefazedone	0.984		clindamycin	0.926
cefazolin	0.979		clometocillin	0.953
cefbuperazone	0.984		clomocycline	0.982
cefcapene pivoxil	0.983		cloxacillin	0.935
cefclidin(a,i,j)	0.985		cyclacillin	0.960
cefdinir(e,i)	0.984		dibekacin	0.952
cefditoren	0.984		dichloramine	0.253
cefepime	0.982		dicloxacillin	0.983
cefetamet	0.983		difloxacin	0.835
cefixime	0.984		diphenicillin sodium	0.767
cefmenoxime	0.984		doxycycline	0.981
cefmetazole	0.984		enoxacin	0.915
cefminox	0.985		enrofloxacin	0.630
cefodizime	0.985		epicillin	0.963
cefonicid	0.984		fenbenicillin	0.967
ceforanide	0.974		fleroxacin	0.980
cefotiam	0.985		flomoxef	0.985
cefoxitin	0.984		florfenicol	0.955
cefozopran	0.982		floxacillin	0.983
cefpimizole	0.985		fortimicin a	0.978
cefpiramide	0.985		fortimicin b	0.700
cefpirome	0.984		furaltadone	0.901
cefpodoxime proxetil	0.985		gentamicin c1	0.850
cefprozil	0.902		gentamicin c2	0.940
cefroxadine	0.970		gentamicin c3	0.956
cefsulodin	0.982		grepafloxacin	0.862
ceftazidime	0.984		guamecycline	0.977
cefteram	0.979		imipenem	0.577
ceftezole	0.984		isepamicin	0.985
ceftizoxime	0.984		kanamycin a	0.962
cefuroxime	0.980		kanamycin b	0.976
cefuzonam	0.985		kanamycin c	0.971
cephacetrile sodium	0.982		lenampicillin	0.985
cephalexin	0.847		lincomycin	0.907
cephaloglycin	0.951		lomefloxacin	0.946
cephaloridine	0.960		loracarbef	0.862
cephalosporin c	0.976		lymecycline	0.978

Table 3. Cont.

Name	Output		Name	Output
meclocycline	0.984		propicillin	0.814
meropenem	0.977		quinacillin	0.984
methacycline	0.983		ribostamycin	0.965
methicillin sodium	0.951		rifamide	0.979
mezlocillin	0.976		rifamycin sv	0.984
micronomicin	0.966		rifaximin	0.984
miloxacin	0.786		ritipenem	0.977
moxalactam	0.984		rolitetracycline	0.979
n2-formylsulfisomidine	0.919		rosoxacin	0.265
n4-sulfanilylsulfanilamide	0.980		rufloxacin	0.975
nadifloxacin	0.658		salazosulfadimidine	0.970
nafcillin sodium	0.919		sancycline	0.980
nalidixic acid	0.268		sisomicin	0.909
neomycin a(c,i,j)	0.983		sparfloxacin	0.975
neomycin b(a,d,h,i)	0.981		spectinomycin	0.628
netilmicin	0.938		succinylsulfathiazole	0.977
nifuradene	0.600		sulbenicillin	0.884
nifuratel	0.980		sulfabenzamide	0.895
nifurfoline	0.963		sulfacetamide	0.955
nifurprazine	0.267		sulfachlorpyridazine	0.915
nifurtoinol	0.694		sulfachrysoidine	0.975
nitrofurantoin	0.291		sulfacytine	0.971
norfloxacin	0.523		sulfadiazine	0.937
N-sulfanilyl-3,4-xylamide	0.956		sulfadicramide	0.933
ofloxacin	0.972		sulfadimethoxine	0.958
oxytetracycline	0.984		sulfadoxine	0.965
panipenem	0.939		sulfaethidole	0.918
paromomycin	0.984		sulfaguanidine	0.904
pasiniazide	0.236		sulfaguanol	0.943
pazufloxacin	0.926		sulfalene	0.938
pefloxacin	0.563		sulfaloxic acid	0.857
penamecillin	0.636		sulfamethazine	0.912
penethamate hydriodide	0.704		sulfamethizole	0.759
penicillin G potassium	0.848		sulfamethomidine	0.940
penicillin N	0.901		sulfamethoxazole	0.908
penicillin O	0.978		sulfamethoxypyridazine	0.912
penicillin V	0.912		sulfamidochrysoidine	0.952
phenethicillin potassium	0.822		sulfamoxole	0.954
phthalylsulfathiazole	0.976		sulfanilamide	0.653
pipacycline	0.921		sulfanilic acid	0.841
pipemidic acid	0.882		sulfanilylurea	0.938
piperacillin	0.982		sulfaphenazole	0.929
piromidic acid	0.696		sulfaproxyline	0.957
pivampicillin	0.916		sulfapyrazine	0.934
pivcefalexin	0.946		sulfathiazole	0.873
p-nitrosulfathiazole	0.893		sulfathiourea	0.849

Table 3. Cont.

Name	Output		Name	Output
sulfisomidine	0.909		bamipine	0.036
sulfisoxazole	0.963		biclofibrate	0.247
sultamicillin	0.983		befunolol	0.252
talampicillin	0.911		benfluorex	0.258
temocillin	0.985		benorylate	0.259
tetracycline	0.983		benserazide	0.259
tetroxoprim	0.837		benzitramide	0.259
thiamphenicol	0.942		benzotropine mesylate	0.000
ticarcillin	0.983		benzpiperylon	0.000
tigemonam	0.985		benzydamine	0.000
trimethoprim	0.739		bermoprofen	0.257
trospectomycin	0.850		betaxolol	0.174
trovafloxacin(b)	0.960		bevantolol	0.154
non-antibiotics			bevonium methyl sulfate	0.032
2-amino-4-picoline	0.258		bezafibrate	0.256
5-bromosalicylic acid acetate	0.258		binifibrate	0.319
5-nitro-2propoxyacetanilide	0.280		bisoprolol	0.184
acecarbromal	0.259		bitolterol	0.004
aceclofenac	0.431		bucloxic acid	0.258
acefylline(c,d,e,g)	0.841		bopindolol	0.001
acetaminophen(b,i)	0.258		bromfenac	0.258
acetanilide	0.258		bromisovalum	0.258
acetazolamide	0.023		bromodiphenhydramine	0.057
acetophenazine	0.265		brompheniramine	0.006
acetylsalicylic acid	0.258		bucetin	0.247
acrivastine	0.260		bucolome	0.253
ahistan	0.000		bucumolol	0.256
albuterol	0.258		bufetolol	0.157
alclofenac	0.258		bufexamac	0.258
alminoprofen	0.256		bufuralol	0.008
alphaprodine	0.106		bumadizon	0.205
alprenolol	0.239		bunitrolol	0.258
aminochlorthenoxazin	0.257		butabarbital	0.258
aminopyrine	0.000		butaclamol	0.123
amosulalol	0.078		butallylonal	0.262
amtolmetin guacil	0.001		butanilicaine	0.206
anileridine	0.262		butibufen	0.255
antipyrine	0.017		butidrine hydrochloride	0.183
antrafenine	0.283		butoctamide	0.252
apazone	0.001		butofilolol	0.256
apronalide	0.258		caffeine	0.159
arotinolol	0.293		capuride	0.257
atenolol	0.258		carazolol	0.027
atropine	0.258		carbamazepine	0.015
bambuterol	0.032		carbidopa	0.259
bamifylline	0.290		carbinoxamine	0.066

Table 3. Cont.

Name	Output		Name	Output
carbiphene	0.258		diethylbromoacetamide	0.257
carbocloral	0.313		difenamizole	0.006
carbromal	0.257		difenpiramide	0.009
carbuterol	0.258		diflunisal	0.258
carfimate	0.258		dilevalol	0.255
carphenazine	0.263		dioxadrol	0.000
carprofen	0.258		dipyrocetyl	0.315
carsalam	0.258		dipyrone	0.041
carteolol	0.259		disulfiram	0.001
carvedilol	0.000		doxefazepam	0.270
celiprolol	0.211		doxofylline	0.629
cetamolol	0.245		doxylamine(b,f,g,i)	0.000
cetirizine	0.261		droperidol	0.259
chlorhexadol	0.288		droxicam	0.022
chlorobutanol	0.258		dyphylline	0.410
chloropyramine	0.050		ectylurea	0.244
chlorothen	0.070		embramine	0.122
chlorpheniramine	0.095		emorfazone	0.010
chlorprothixene	0.017		enfenamic acid	0.256
chlorthenoxacin			enprofylline	0.246
(chlorthenoxazine)	0.258		epanolol	0.258
chlorcyclizine	0.078		ephedrine	0.229
cinchophen	0.251		epirizole	0.002
cinmetacin	0.248		eprozinol	0.237
cinnarizine	0.388		estazolam	0.000
cinromida	0.197		etafedrine	0.179
ciprofibrate	0.251		etamiphyllin	0.118
clemastine	0.039		etaqualone	0.000
clenbuterol	0.234		eterobarb	0.001
clidanac	0.258		etersalate	0.260
clinofibrate	0.282		ethenzamide	0.243
clofibric acid	0.256		ethinamate	0.258
clometacin	0.292		ethoheptazine	0.000
clometiazol	0.255		ethoxazene	0.248
clonixin	0.254		etodolac	0.259
clopirac	0.257		etofibrate	0.260
cloranolol	0.247		etofylline	0.266
clordesmetildiazepam	0.257		etomidate	0.000
clorprenaline	0.249		etymemazine	0.002
clothiapine	0.003		felbinac	0.258
clozapine	0.051		fenadiazole	0.230
codeine	0.062		fenbufen	0.258
cropropamide	0.002		fenclofenac	0.259
crotethamide	0.035		fenethazine	0.000
deserpidine	0.005		fenofibrate	0.254
diclofenac	0.262		fenoprofen	0.258

Table 3. Cont.

Name	Output		Name	Output
fenoterol	0.258		lornoxicam	0.031
fentanyl	0.066		loxapina	0.004
fentiazac	0.259		loxoprofen	0.258
floctafenine	0.266		mazindol(i)	0.162
flufenamic acid	0.259		meclofenamic acid(f)	0.276
fluoresone	0.459		mecloqualone	0.000
fluphenazine	0.260		medibazine	0.004
flupirtine	0.260		medrylamine	0.001
fluproquazone	0.258		meparfynol	0.258
flurazepam	0.010		mepindolol	0.211
flurbiprofen	0.258		meprobamate	0.259
fluspirilene	0.259		mequitazine	0.001
flutropium bromide	0.259		methafurylene	0.000
formoterol	0.259		methaphenilene	0.000
fosazepam	0.258		methotrimeprazine	0.002
fusaric acid	0.258		methoxyphenamine	0.000
gemfibrozil	0.248		methyldopa	0.258
gentisic acid	0.258		methyltyrosine	0.256
glafenine	0.259		methyprylon	0.232
glucametacin	0.335		metiapine	0.002
glutethimide	0.258		metipranolol	0.258
haloperidide	0.259		metofoline	0.094
haloperidol	0.258		metoprolol	0.179
hexapropymate	0.258		metron	0.275
hexobarbital	0.274		mexiletine	0.251
hexoprenaline	0.258		mofezolac	0.340
histapyrrodine	0.004		molindone	0.000
hydroxyethylpromethazine			moperone	0.259
(N-Hydroxyethylpromethazine)	0.261		moprolol	0.213
hydroxyzine	0.261		morazone	0.000
ibufenac	0.258		morphine	0.289
ibuprofen	0.258		moxastine	0.000
ibuproxam	0.258		nadoxolol	0.258
indenolol	0.179		naproxen	0.256
indomethacin	0.323		narcobarbital	0.265
ipratropium bromide	0.259		nefopam	0.000
isoetharine	0.258		niceritrol	0.981
isofezolac	0.183		nicoclonate	0.095
isonixin	0.125		nicofibrate	0.214
isopromethazine	0.000		nifenalol	0.256
isoxicam	0.003		nifenazone	0.000
ketoprofen	0.250		niflumic acid	0.260
ketorolac	0.259		nimetazepam	0.512
labetalol	0.252		nipradilol	0.611
lefetamine	0.068		nitrazepam	0.337
lorazepam	0.268		nordiazepam	0.254

Table 3. Cont.

Name	Output		Name	Output
novonal	0.255		propyphenazone	0.000
octopamine	0.258		protokylol	0.260
orphenadrine	0.000		proxibarbital	0.262
oxaceprol	0.259		proxyphylline	0.210
oxametacine	0.284		pyrilamine	0.000
oxanamide	0.254		pyrrobutamine	0.000
oxaprozin	0.259		quazepam	0.331
oxitropium bromide	0.265		ramifenazone	0.000
oxprenolol	0.221		reproterol	0.296
oxypertine	0.000		rimiterol	0.258
paramethadione	0.258		ronifibrate	0.259
parsalmide	0.259		salacetamide	0.258
p-bromoacetanilide	0.258		salicylamide	0.257
pemoline	0.258		salicylamide O-acetic acid	0.258
penbutolol	0.099		salsalate	0.258
penfluridol	0.259		salverine	0.000
perisoxal	0.034		scopolamine	0.278
perphenazine	0.284		secobarbital	0.257
phenacemide	0.258		setastine	0.035
phenacetin	0.247		simetride	0.028
phenoperidine	0.191		simfibrate	0.259
phenopyrazone	0.243		simvastatin	0.355
phenylbutazone	0.000		sotalol	0.013
phenyltoloxamine(a,c,g)	0.000		soterenol	0.099
pindolol	0.055		sulfinalol	0.062
pipebuzone	0.001		sulpiride	0.017
piperacetazine	0.261		suprofen	0.258
piperidione	0.253		talastine	0.000
piperylone	0.000		talinolol	0.245
pirbuterol	0.259		talniflumate	0.399
pirifibrate(g,h)	0.258		temazepam	0.207
piroxicam	0.013		tenoxicam	0.008
pirprofen	0.258		terbutaline	0.258
p-lactophenetide	0.257		tertatolol	0.129
p-methyldiphenhydramine	0.000		tetrabarbital	0.257
pravastatin	0.438		thenaldine	0.000
prazepam	0.008		thenyldiamine	0.000
primidone	0.133		theobromine	0.251
probucol	0.000		theofibrate(b,f,i)	0.435
procaterol	0.260		theophylline(f,h,i,j)	0.224
proglumetacin	0.292		thioridazine	0.003
prolintane	0.024		thiothixene	0.003
promazine	0.000		thonzylamine	0.001
pronethalol	0.237		tiaprofenic acid	0.258
propanolol	0.067		timolol	0.030

Table 3. Cont.

Name	Output		Name	Output
toliprolol	0.127		tripelennamine	0.000
tolmetin	0.254		triprolidine	0.000
tolpropamine	0.001		tulobuterol	0.169
tretoquinol	0.418		viminol	0.028
triazolam	0.003		vinylbital	0.258
triclofos	0.276		xenbucin	0.256
trifluoperazine	0.298		xibenolol	0.148
trifluperidol	0.259		zolamine	0.035
trimethadione	0.258		zomepirac	0.263
triparanol	0.248			

Table 4. Compounds of the testing set and the corresponding output values from the trained neural network with three hidden nodes.

Name	Output		Name	Output
antibiotics			butacetin	0.147
amoxicillin	0.152		chlorpromazine	0.169
ampicillin	0.728		ciramadol	0.150
cefoperazone	0.997		clocinizine	0.125
cefotaxime	0.999		clofibrate	0.142
cefotetan	0.568		diazepam	0.997
cefteram	0.999		diphenhydramine	0.125
ceftriaxone	0.999		diphenylpyraline	0.101
ciprofloxacin	0.999		esmolol	0.151
demeclocycline	0.999		ethclorvinol	0.047
flumequine	0.998		feprazone	0.118
hetacillin	0.992		flunitrazepam	0.069
mafenide	0.999		fosfosal	0.134
metampicillin	0.978		indoprofen	0.287
minocycline	0.984		isoproterenol	0.151
nifurpirinol	0.998		levobunolol	0.150
noprylsulfamide	0.998		lovastatin	0.151
oxacillin	0.999		mabuterol	0.149
oxolinic acid	0.991		mefenamic acid	0.097
sulfamerazine	0.999		mefexamide	0.000
sulfametrole	0.999		meperidine	0.146
sulfanitran	0.998		mephobarbital	0.160
sulfaperine	0.997		methapyrilene	0.000
temafloxacin	0.987		nadolol	0.151
thiazolsulfone	0.994		pheniramine	0.134
tobramycin	0.994		phenocoll	0.000
tosufloxacin	0.995		phenyramidol	0.000
non-antibiotics			pimozide	0.029
acetaminosalol	0.110		practolol	0.152
acetobutolol	0.150		proheptazine	0.149
aminopropylon	0.000		propacetamol	0.166
benoxaprofen	0.150		sulindac	0.975
brotizolam	0.004		talbutal	0.063
bupranolol	0.144			

Table 5. Output values from the neural network for the validation set's antibiotics.

Compound	Structural formula	Prediction
286547	3a	0.984
286724	3c	0.985
286725	3c	0.985
286726	3c	0.985
286727	3c	0.985
286728	3c	0.985
286847	3b	0.915
286848	3b	0.914
287132	3d	0.985
287133	3d	0.985
287135	3d	0.985
287136	3d	0.985

These results demonstrate that the developed ANN-based binary classifier of antibacterial activity is adequate and can be considered an effective tool for 'in silico' antibiotics discovery. The results also demonstrate that the inductive parameters readily accessible by formulas (1)-(11) from atomic electronegativities, covalent radii and interatomic distances can produce a variety of useful QSAR descriptors to be used '*in silico*' chemical research.

Conclusions

The results of the present work demonstrate that a variety of atomic, substituent and molecular properties which can be computed within the framework of our previous models for inductive and steric effects, inductive electronegativity and molecular capacitance represent a powerful arsenal of 3D QSAR descriptors for modern '*in silico*' drug research. Using only 34 inductive descriptors with no additional independent parameters we have achieved 93% correct classification of compounds with- and without antibacterial activity. The introduced inductive descriptors possess a number of important merits: they are 3D- and stereo- sensitive, can be easily computed from fundamental properties of bound atoms and molecules and possess much defined physical meaning. The developed ANN-based model for antibiotic-likeness prediction can be used as a powerful QSAR tool for filtering through the collections of chemical structures to discover novel antibiotic leads.

Methods

The names of the chemical compounds from the dataset from [27] have been translated into SMILES records and MOL files using the *ChemIDPlus* online service [45] and the MOE package [32]. 50 inductive descriptors have been calculated using by the SVL scripts – a specialized language of the MOE package. The interatomic distances have been calculated by the MOE from the molecular structures optimized with the MMFF94 force-field [46]. The atomic types have been assigned according to the name, valent state and a formal charge of atoms as it is defined within the MOE. The parameters of the corresponding atomic electronegativities and covalent radii have been taken from

our works [5, 8]. The inductive QSAR descriptors used in the study have been normalized into the range [0.0÷1.0] and the non-overlapping training and testing sets have been randomly drawn by the customized Java scripts. The training and testing of the neural networks has been conducted using the Stuttgart Neural Network Simulator [47]. The training was performed through the feed-forward back-propagation algorithm with the weight decay and pattern shuffling. The values of initial rates were randomly assigned in a range [0.0÷1.0], the learning rate has been set to 0.8 with the threshold 0.10.

References

1. Kubinyi, H.; Folkers, G.; Martin, Y.C. Eds. *3D QSAR in Drug Design*; Kluwer: Dordrecht, **2002**.
2. Truhlar, D.G.; Howe, W.J.; Hopfinger, A.J. Eds *Rational Drug Design*; Springer: Berlin, **1999**.
3. Karelson, M. *Molecular Descriptors in QSAR/QSPR*; Wiley: New York, **2000**; p. 448.
4. Exner, O. *Correlation Analysis of Chemical Data*: Kluwer: Dordrecht, **1988**.
5. Cherkasov, A.R.; Galkin, V.I.; Cherkasov, R.A. *J. Phys. Org. Chem.* **1998**, *11*, 437.
6. Cherkasov, A.R.; Galkin, V.I.; Cherkasov, R.A. *J. Molec. Struct. (Theochem)* **1999**, *489*, 43.
7. Cherkasov, A.R.; Galkin, V.I.; Cherkasov, R.A. *J. Molec. Struct. (Theochem)* **2000**, *497*, 115.
8. Cherkasov, A. *J. Chem. Inf. Comp. Sci*. **2003**, *43*, 2039.
9. Babij C.; Poe A.J. *J. Phys. Org. Chem*. **2004**, *17*, 162.
10. Galkin, V.I.; Sayakhov, R.D.; Cherkasov, R.A. *Russ. Chem. Rev.* **1991**, *60*, 1617.
11. Cherkasov, A.; Jonsson, M. *J. Chem. Inf. Comp. Sci*. **1998**, *38*, 1151.
12. Cherkasov, A.; Jonsson, M. *J. Chem. Inf. Comp. Sci*. **1999**, *39*, 1057.
13. Cherkasov, A.R.; Jonsson, M.; Galkin, V.I. *J. Mol. Graph. Model.* **1999**, *17*, 28.
14. Cherkasov, A.; Jonsson, M. *J. Chem. Inf. Comp. Sci*. **2000**, *40*, 1222.
15. Cherkasov, A.; Sprous, D.; Chen, R. *J. Phys. Chem. A.* ***2003***, *107*, 9695.
16. Galkin, V.I.; Cherkasov, A.R.; Cherkasov, R.A. *Phosphorus, Silicon, Sulphur* **1999**, *146*, 329.
17. Byvalov, E.; Fechner, U.; Sadowski, J.; Schneider, G. *J. Chem. Inf. Comp. Sci*. **2003**, *43*, 1882.
18. Zernov, V.; Balakin, K.V.; Ivaschenko, A.A.; Savchuk, N.P.; Pletnev, I.V. *J. Chem. Inf. Comp. Sci*. **2003**, *43*, 2048.
19. Anzali, S.; Barenickel, G.; Cezanne, B.; Krug, M.; Filimonov, D.; Poroikob, V. *J. Med. Chem.* **2001**, *44*, 2432.
20. Murcia-Soler, M.; Perez-Gimenez, F.; Garcia-March, F.J.; Salabert-Salvador, M.T.; Diaz-Villanueva, W.; Castro-Bleda, M.J. *J. Chem. Inf. Comp. Sci*. **2003**, *43*, 1688.
21. Frimurer, T.M.; Bywater, R.; Naerum, L.; Lauritsen, L.N.; Brunak, S. *J. Chem. Inf. Comp. Sci*. **2000**, *40*, 1315.
22. Sadowski, J.; Kubinyi, H. *J. Med. Chem.* **1998**, *41*, 3325.
23. Galvez, J.; de Julian-Ortiz, J.V.; Garcia-Domenech, R. *J. Mol. Graph. Model.* **2001**, *20*, 84.
24. Ajay, A.; Walters, W.P.; Murcko M.A., *J. Med. Chem.* **1998**, *41*, 3314.
25. Jaen-Oltra, J.; Salabert-Salvador, M.T.; Garcia-March, F.J.; Perez-Gimenez, F., Tomas-Vert, F. *J. Med. Chem.* **2000**, *43*, 1143.
26. Garcia-Domenech, R.; de Julian-Ortiz, J.V. *J. Chem. Inf. Comp. Sci*. **1998**, *38*, 445.
27. Tomas-Vert, F.; Perez-Gimenez, F.; Salabert-Salvador, M.T.; Garcia-March, F.J.; Jaen-Oltra, J. *J. Molec. Struct. (Theochem)*. **2000**, *504*, 249.
28. Mishra, R.K.; Garcia-Domenech, R.; Galvez, J. *J. Chem. Inf. Comp. Sci*. **2001**, *41*, 387.

29. Cronin, M.T.D.; Aptula, A.O.; Dearden, J.C.; Duffy, J.C.; Netzeva, T.I.; Patel, H.; Rowe, P.H.; Schultz T.W.; Worth, A.P.; Voutzoulidis, K.; Schuurmann, G. *J. Chem. Inf. Comp. Sci*. **2002**, *42*, 869.
30. Molina, E.; Diaz, H.G.; Gonzalez M.P.; Rodriguez, E.; Uriarte, E. *J. Chem. Inf. Comp. Sci*. **2004**, *44*, 515.
31. Gozalbez, R.; Galvez, J.; Moreno, A.; Garcia-Domenech, R. *J. Pharm. Pharmacol.* **1999**, *51*, 111.
32. *Molecular Operational Environment*, **2004**, by Chemical Computation Group Inc., Montreal, Canada.
33. Zupan, J.; Gasteiger, J. *Neural Networks in Chemistry and Drug Design,* 2nd Ed.; Wiley: New York, **1999**.
34. Dastidar, S.D.; Ganguly, K.; Chaudhuri, K.; Chakrabarty, A.N. *Int. J. Antimicrob. Agents* **2000**, *14*, 249.
35. Annadurai, S.; Basu, S.; Ray, S.; Dastidar, S.D.; Chakrabarty, A.N. *Indian J. Exp. Biol*. **1998**, *36*, 86.
36. Dastidar, S.D.; Saha, P.K.; Sanymat, B.; Chakrabarty, A.N. *J. Appl. Bact.* **1976**, *42*, 209.
37. Dastidar, S.D.; Jairaj, J.; Mookerjee, M.; Chakrabarty, A.N. *Acta Microbiol. Immun. Hung.* **1997**, *44*, 241.
38. Molnar, J.; Mandi, Y.; Kiraly, J. *Acta Microbiol. Immun. Hung.*, **1976**, *23*, 45.
39. Kristiansen, J.E. *Acta Path. Microbioil. Scand. Sect. B*. **1979**, *87*, 317.
40. Kristiansen, J.E.; Mortensen, I. *Pramocol. Toxicol*. **1987**, *60*, 100.
41. Dastidar, S.D.; Chaudhuri, K.; Annadurai, S.; Ray, S.; Mookerjee, M.; Chakrabarty, A.N. *J. Chemother*. **1995**, *7*, 201.
42. Dash, S.K.; Dastidar, S.D.; Chaudhuri, K. *Ind. J. Exp. Biol.* **1977**, *15*, 324.
43. Dastidar, S.D.; Mondal, U.; Niyogi, S.; Chakrabarty, A.N. *Ind. J. Med. Res.* **1986**, *84*, 142.
44. *Drug Data Report*, **2000**, *22*, 530.
45. *ChemIDPlus* database: http://chem.sis.nlm.nih.gov/chemidplus/
46. Halgren, T.A. *J. Comp. Chem.* **1996**, *17*, 490.
47. *SNNS: Stuttgart Neural Network Simulator, Version 4.0*; University of Stuttgart: Stuttgart**, 1995**.

© 2005 by MDPI (http://www.mdpi.org). Reproduction is permitted for noncommercial purposes.